# Molecular Complexity Favors the Evolution of Ribopolymers[†]

Fabiana Ciciriello,[‡,§] Giovanna Costanzo,[‡,||] Samanta Pino,[‡,§] Claudia Crestini,[‡,⊥] Raffaele Saladino,[‡,#] and Ernesto Di Mauro*[,‡,§]

*Dipartimento di Genetica e Biologia Molecolare, Università di Roma "Sapienza", 00185 Rome, Italy, Istituto di Biologia e Patologia Molecolari, Consiglio Nazionale delle Ricerche (CNR), Rome 00185, Italy, Dipartimento di Scienze e Tecnologie Chimiche, Università "Tor Vergata", Rome 00133, Italy, and Dipartimento ABAC, Università della Tuscia, Viterbo 01100, Italy*

*Received October 18, 2007; Revised Manuscript Received December 21, 2007*

ABSTRACT: We have explored the stability of selected ribo oligomers in water and have determined the physical−chemical conditions in which the key 3′-phosphoester bond is more stable when embedded in the polymer than when present in the monomer. In these conditions, the spontaneous formation and the survival of ribo polymers are potentially favored. A narrow pH range was identified in which complex sequences resist degradation markedly more than monotonous ones, thus potentially favoring the evolution of sequence-based genetic information. Given that the founding property of a polymer is to maintain its polymeric form and its sequence information, these findings support the view that the evolution of pregenetic molecular information occurred based on intrinsic properties of nucleic polymers.

The first property of a polymer is to maintain its polymeric form. In prebiotic nonenzymatic polymerizations, the problem of the standard-state Gibbs free-energy change ($\Delta G^{\circ\prime}$) (*1*) defines a critical thermodynamic scenario: polymerization processes entailing the release of water are, in water, thermodynamically forbidden. Alternative possibilities could have consisted in the dry state, mineral surface-mediated polymerization and/or in the polymerization in nonaqueous media. Whatever solution actually took place, the earliest polymers once formed had at one stage adapted to the aqueous environment into which they operate at present. Does an intrinsic property of nucleic polymers exist, allowing this evolutionary key adaptation?

For an initial understanding of the early steps of these processes, we have identified one problem and one condition, focusing on the resistance of nucleic acid phosphoester bonds to hydrolysis. We have chosen the simplest possible experimental approach: lyophilized polymers were solubilized, and their fate upon solubilization was analyzed. To bring the problem under manageable complexity, we asked a minimalist question: which are the intrinsic endurance properties of one nucleic acid (RNA) when brought in solution in one solvent (water)? These properties were analyzed in a representative set of simple sequences, in a large range of pH and temperature conditions, for the appropriate lapses of time. This experimental setup has interest per se. In addition, it models the hypothesized passage from a dry nonaqueous to an aqueous condition.

The purpose of the analysis was to verify whether properties come about in the polymer, which are not present in the monomers, providing with kinetic resistance the bonds that are more sensitive to hydrolysis. If these bonds are more resistant in the polymer relative to the same bonds in the monomer, one reason for the very existence of the polymeric form would be established. Additionally, if complex sequences are more resistant than monotonous polymers, evolution of complexity would have been favored.

Degradation of RNA in water occurs by transesterification of phosphodiester bonds, an intensively studied and well-described process (*2–4*). Despite the detailed knowledge of RNA transesterifications, we have found that kinetic aspects of the process were not previously described, which provide part of the solution to the unanswered question: how did informational polymers come to existence?

## EXPERIMENTAL PROCEDURES

Adenine, ribose, ribose 5′-monophosphate, adenosine, adenosine 5′-monophosphate (5′-AMP),[1] adenosine 3′-monophosphate (3′-AMP), adenosine 2′-monophosphate (2′-AMP), adenosine 2′−3′-cyclic monophosphate (2′−3′-cAMP), adenosine 3′−5′-cyclic monophosphate (3′−5′-cAMP), cytosine, cytidine, cytosine 3′-monophosphate (3′-CMP), cytosine 2′-monophosphate (2′-CMP), and cytosine 5′-monophosphate (5′-CMP) were from Sigma Aldrich and of analytical grade.

[†] This work was supported by the Italian Space Agency Project MoMa, I/015/07/0 and by MURST-CNR "Progetto Genomica Funzionale" to Ernesto Di Mauro.

* To whom correspondence should be addressed: Dipartimento di Genetica e Biologia Molecolare, Università "Sapienza" di Roma, P.le Aldo Moro, 5, Rome 00185, Italy. Telephone: +39-06-49912880. Fax: +39-06-49912500. E-mail: ernesto.dimauro@uniroma1.it.

[‡] These authors contributed equally to this work.

[§] Università di Roma "Sapienza".

[||] Consiglio Nazionale delle Ricerche (CNR).

[⊥] Università "Tor Vergata".

[#] Università della Tuscia.

[1] Abbreviations: 5′-AMP, adenosine 5′-monophosphate; 3′-AMP, adenosine 3′-monophosphate; 2′-AMP, adenosine 2′-monophosphate; 2′−3′-cAMP, adenosine 2′−3′-cyclic monophosphate; 3′−5′-cAMP, adenosine 3′−5′-cyclic monophosphate; 3′-CMP, cytosine 3′-monophosphate; 2′-CMP, cytosine 2′-monophosphate; 5′-CMP, cytosine 5′-monophosphate; HPLC, high-performance liquid chromatography.

10.1021/bi7021014 CCC: $40.75 
Published on Web 01/26/2008

*RNA*. The degradation of RNA was analyzed in water and in formamide on Poly $A_{24}$, Poly $A_{12}C_{12}$, and P1 RNA. Poly A is a homogeneous stretch of 24 A residues, Poly $A_{12}C_{12}$ is a stretch of 5′-$A_{12}C_{12}$-3′ residues. P1 is an oligo with the sequence 5′-GGAAACGUAUCCUUUGGGAG-3′ (*5*). They were all purchased from Dharmacon and provided in the standard lyophilized form.

*Half-Lives of the 3′-Phosphoester Bond in 3′-AMP*. The half-life of the 3′-phosphoester bond in 3′-AMP and 3′-CMP was calculated at the pH and temperature conditions indicated where appropriate and as specified below, following a procedure detailed in ref *46*.

Commercial distilled water was further purified by tridistillation−deionization with a MilliQ Advantage A10 or with a Sartorius ARIUM 611 VF apparatus. Pure or 10 mM Tris-HCl-buffered water were pretreated for 2 h at the temperature of the assay to be performed, a period of time sufficient to reach and maintain the temperature-specific pH. The temperature-stabilized pH values (determined on a Beckman Ø 40 pH meter) are given throughout.

Samples were resuspended at a 0.025 M final concentration in water or in the appropriate formamide reaction medium (usually in 0.5–1.0 mL) and incubated at various temperatures (20, 30, 50, 60, 70, 80, or 90 °C) at the indicated pH values for the appropriate periods of time. Aliquots (5 μL) were diluted to a final concentration of 50% formamide in a final volume of 10 μL and injected into a Supelcosil LC-18-T 3 μm high-performance liquid chromatography (HPLC) column (Supelco), 15 cm × 4.6 mm. Elution was performed at a flow rate of 2 mL/min at room temperature with methanol/30 mM ammonium phosphate at pH 5.3 (2.5/97.5), UV 254 nm, on a HPLC Beckman System Gold instrument. Identification of the peaks was performed by a comparison to real samples. Several examples of the graphical representation of the kinetics of degradation of nucleosides and nucleotides as determined by this method are in refs *46* and *47*. Half-lives were determined by standard graphical procedures.

*RNA Labeling and Handling. RNA 5′ Labeling*. A total of 10 μmol of the oligo RNA were labeled with [$\gamma$-$^{32}$P]ATP using polynucleotide kinase (Roche Applied Science). The oligo was then purified on a 16% denaturing acrylamide (19:1 acrylamide/bisacrylamide) gel. After elution, the residual polyacrylamide was removed by a NuncTrap Probe purification column (Stratagene). At this point, the RNA, suspended in 160 μL of STE buffer [100 mM NaCl, 20 mM Tris-HCl at pH 7.5, and 10 mM ethylenediaminetetraacetic acid (EDTA)] was precipitated by the addition of glycogen (20 μg in 1 μL of biodistilled sterile water) and 3 volumes of ethanol, kept overnight at −20 °C, centrifuged (Savant, 20 000 rpm, 10 min, room temperature, and environmental atmospheric pressure), washed once with 70% ethanol/water, and centrifuged as above. The pellet was suspended in $H_2O$, distributed in 15 μL aliquots, immediately frozen, and conserved at −20 °C. Typically, one aliquot was used for each experiment and 2 pmol (typically 30 000 cpm) of RNA was processed for each sample.

*Ribo Oligonucleotide Degradation Protocols and Analyses*. 5′-Labeled oligonucleotides were treated at the temperature, time, and solution conditions indicated, where appropriate. To stop the reactions carried out in water (pH 5.5 at 90 °C), the sample (typically 15 μL) was diluted and precipitated with 3 vol of 96% ethanol, 0.3 M sodium acetate final concentration at pH 7.5, and 20 μg of glycogen. To stop the reactions carried out in formamide, a solution of $5 \times 10^{-4}$ M (final concentration) of tetrasodium pyrophosphate (Sigma) dissolved in water (final pH 7.5) was added to a final volume of 40 μL. The samples were vortexed for 1 min and then centrifuged at 13 000 rpm for 20 min. This procedure was performed twice. The supernatant was ethanol precipitated as above, resuspended in 5 μL of formamide buffer, heated for 2 min at 65 °C, and loaded on a 16% denaturing polyacrylamide gel (19:1 acrylamide/bisacrylamide). For these methods, see also ref *46*.

*Half-Lives of the Bonds in the Ribo Oligonucleotide*. For oligonucleotides, the half-lives of the phosphoester bonds were determined from the rate of disappearance of the band representing the intact 20- or 24-mer molecule.

The cleavage of RNA normally requires participation of the 2′-OH group as an internal nucleophile (*6* and refs therein), by two "nucleophilic cleavage" events: the transesterification and hydrolysis reactions. During the transesterification, the 2′-OH nucleophile attacks on tetrahedral phosphorus, affording a 2′−3′-cyclic monophosphate, which in turn is hydrolyzed to a mixture of 3′- and 2′-phosphate monoesters. On the basis of this known mechanism and of common experimental experience, we assumed that the cleavage of the 3′-phosphoester bond is largely more effective that the cleavage of the 5′ one and that, for practical calculation purposes, the 5′-phosphoester bond is not cleaved.

The half-life of the oligonucleotide was determined with a standard graphical procedure from plots of the percent disappearance of the intact full-length molecules, the half-life value corresponding to the time value at which 50% of the full-length molecules had disappeared. Given that one disappearing molecule *a priori* represents one cleavage, the half-life of a 3′-phosphoester bond in the ribo oligonucleotide is given by the half-life of the oligonucleotide × 19 (that is, the number of 3′-phosphoester bonds in the P1 20-mer) or × 23 (that is, the number of 3′-phosphoester bonds on the Poly $A_{24}$ and Poly $A_{12}C_{12}$ 24-mer oligos), respectively.

## RESULTS

We have determined the half-life of the 3′-phosphoester bond when present in the ribo monomer 3′-AMP or 3′-CMP (section 1) or in oligonucleotides (section 2), as a function of the pH and temperature. The results are compared (section 3).

*1. 3′-Phosphoester Bond in 3′-AMP and 3′-CMP. 3′-AMP*. The cleavage rate of the 3′-phosphoester bond of 3′-AMP was determined by incubation in water at 90 °C at the Tris-HCl-buffered pH values of 3.37, 3.72, 4.31, 4.98, 5.26, 5.34, 5.60, 5.92, 6.48, 7.21, 7.69, 8.25, 8.57, 8.73, and 9.02. The treatment lasted up to 92 h, and the products were analyzed by HPLC at the time intervals indicated in Figure 1 (abscissa). This figure (which shows selected examples of the larger data set reported in Figure 2) illustrates the degradation of 3′-AMP (percent, ordinate) as a function of time (abscissa) and of the pH (indicated in the central upper part of each panel). The upper panel on the right side provides the interpretation key. The blue letters indicate the starting compound; in this case, ribose (R) bound to the base (B) adenine and to the phosphate (P). The cleavage (arrow)

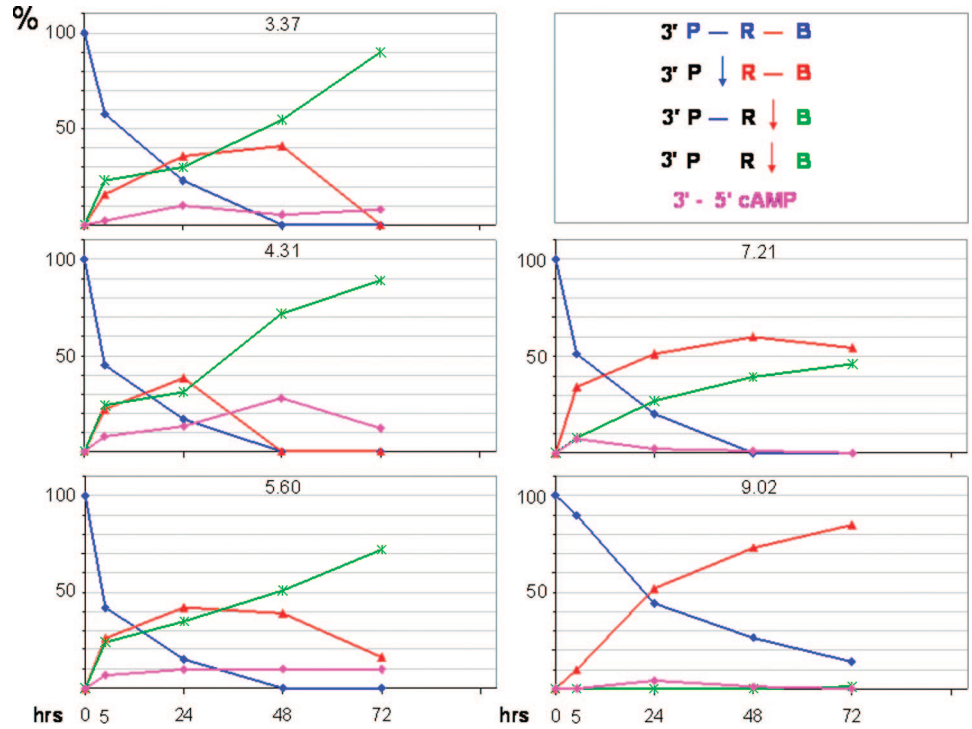


FIGURE 1: Degradation kinetics of 3′-AMP as a function of the pH indicated in each panel, HPLC analysis. Blue, nucleotide; red, nucleoside; green, base. The ribose and ribose−phosphate moieties are not detected in the HPLC analysis and are indicated in black. Also see the text in section 1. The line connecting the experimental points, here and in the following plots, has no mathematical meaning. It is given only to facilitate identification.

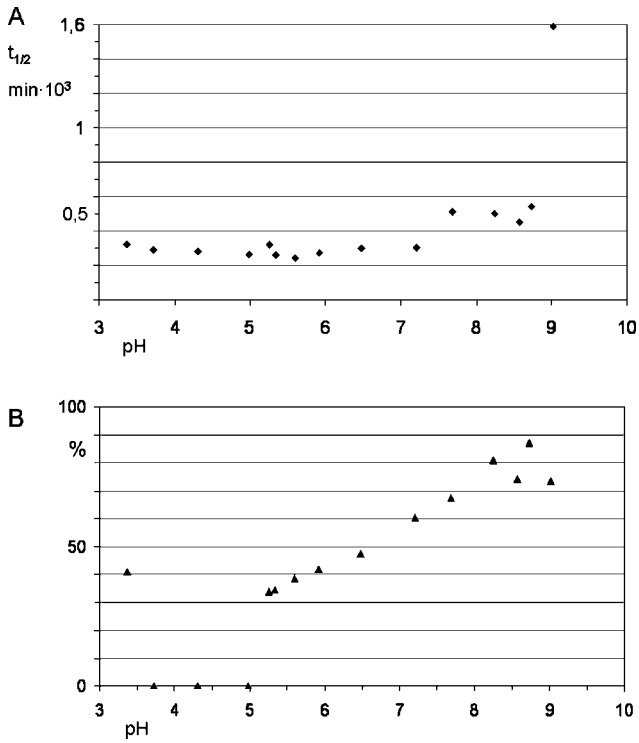


FIGURE 2: (A) Half-life of 3′-AMP as a function of the pH. The half-life values (ordinate) were calculated in water, at 90 °C, by HPLC kinetic analysis as exemplified in Figure 1, at the pH values indicated (abscissa). (B) Yield of adenosine as a function of the pH, in water, at 90 °C. The amount of adenosine (reported as a percentage of the total input, ordinate) was calculated from the same analyses reported in Figure 1 and in A, at the pH values indicated (abscissa).

of the phosphoester bond (blue) yields the nucleoside (R−B, red) and the phosphate (black). Black indicates compounds that are not detected under these analytical conditions. The cleavage of the glycosidic bond (red) yields adenine (B, green) and ribose−phosphate (R−P, black). 3′−5′-cAMP is magenta.

The results show that 3′-AMP in water at 90 °C has a $t_{1/2} \sim 0.3 \times 10^3$ min. This value is only marginally pH-dependent between pH <3.37 and >8.73, as shown in Figure 2A. The degradation of 3′-AMP occurs by cleavage of the $\beta$-glycosidic and/or the 3′-phosphoester bonds. The first cleavage results in the production of adenine (green), and the latter results in the production of adenosine (red).

The stability of adenosine was measured separately in a similar set of analyses (not detailed) showing that in the whole range of pH values analyzed adenosine was only marginally degraded. Thus, in the degradation of 3′-AMP in water at 90 °C, adenine is mostly produced by depurination of the nucleotide form and not from the adenosine nucleotide deriving from its dephosphorylation. After depurination, the phosphoester bond connecting the ribose and phosphate moieties (which in this analytical setup are not detected) is cleaved by a well-characterized $\beta$-elimination mechanism (*7*).

Figure 2B shows that 3′-AMP depurination is faster between pH >3.72 and <4.98.

At pH values higher than 7.21 (Figure 1), little adenine is formed, showing that in alkaline conditions the $\beta$-glycosidic is protected and that degradation of the nucleotide mostly occurs by high pH-enhanced dephosphorylation. The increase of adenine after 48 h is given by the sum of the adenine formed previously plus the adenine being produced from adenosine until its consumption. The formation of a discrete amount of *bona fide* 3′−5′-cyclic AMP is also observed (magenta). The corresponding peak in the HPLC profile was assigned by a comparison to real sample 3′−5′-cAMP, while 2′-AMP, 3′-AMP, and 2′−3′-cAMP eluted in different

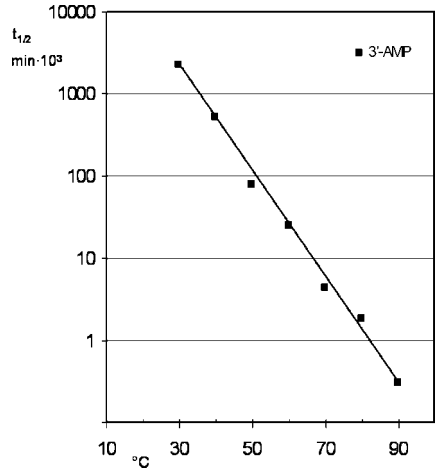


FIGURE 3: Half-life of 3′-AMP in water at pH 5.5 as a function of the temperature. The experimental procedure and analysis are the same as the experiment reported in Figure 1.

positions. This matter is not directly relevant to the scope of this study and was not analyzed further.

In conclusion, the degradation of 3′-AMP is largely a pH-independent process between pH ~3.0 and ~7.0. In this range of values, the contribution of depurination is higher between ~3.7 and ~5.0.

The half-life of 3′-AMP was also determined as a function of the temperature at pH 5.5 in water (Figure 3), showing its steady temperature-dependent increase.

*3′-CMP.* The cleavage rates of the 3′-phosphoester bond of 3′-CMP were determined by a similar set of analyses for the same range of pH values. The results (Figure 4, selected examples) showed that the degradation of 3′-CMP is an essentially pH-independent process and that the cleavage of the $\beta$-glycosidic bond resulting in the production of cytosine is faster than the cleavage of the 3′-phosphoester bond yielding cytidine. Despite this kinetic difference, the quantitative relevance of the two clevages is roughly equivalent. Both cytosine and cytidine are stable in these experimental conditions.

*2. Kinetics of RNA Hydrolysis.* We performed the simple test of measuring the kinetics of degradation of a 5′-labeled RNA in water at various temperatures on the three following oligos: (i) Poly $A_{24}$, (ii) Poly $A_{12}C_{12}$, and (iii) mixed-sequence oligo P1.

Figures 5A, 6A, and 7A show the degradation profiles of Poly $A_{24}$, Poly $A_{12}C_{12}$, and mixed-sequence oligos, respectively, treated at 90 °C as a function of time. Let us examine first the qualitative aspects of the hydrolytic reactions.

*Qualitative Aspects. Poly $A_{24}$.* The pattern of hydrolytic degradation of Poly $A_{24}$ at 90 °C (Figure 5A) shows that the 24-mer was regularly hit by hydrolytic events along its whole length, as shown by the appearance of the ladder-like degradation profiles. After about 6 h of permanence of the RNA in water, degradation started.

The relatively high stability of the Poly A sequence in aqueous solution is well-established (*8–10*). The stability of RNA phosphodiester bonds has repeatedly been associated with the stacking interactions between adjacent bases (*11–13*). Nucleic acid–base stacking is at present an essentially well-understood phenomenon (*14–21*). The possibility that the initial stability of the Poly A oligo toward hydrolysis is a base-stacking-related effect is discussed below.

The upper panel shows the degradation observed in water at pH 5.5 (90 °C). The bottom panel shows the disappearance of full-length molecules of the same oligo at pH 6.2 (90 °C) (discussed in the following section).

*Poly $A_{12}C_{12}$.* The cleavage profile of Poly $A_{12}C_{12}$ (Figure 6) showed that the bipartite oligo molecule behaved toward degradation as two separate entities: the C stretch and the A stretch. The two sequence components did not appreciably affect each other.

In these experimental conditions (water at pH 5.5 and 90 °C), the C-stretch component was rather unstable, its degradation already starting during the handling of the sample (i.e., see the $T_0$ sample, first lane). The intensity of the bands indicating the cleavage products increased from the top toward the limit of the C stretch (the 5′-ApC-3′ border) (Figure 6A). The cleavage pattern depicts the progressively decreasing size of the homogeneous sequence stretch and is compatible with both a multiple independent hit kinetics and/or a cooperative cleavage mechanism. Conformation and thermodynamic properties of oligocytidylic acids are known (*23*). These oligomers possess a single-stranded stacked-base helical conformation at low temperatures and at neutral or alkaline pH (*23*). The standard-state free-energy change obtained at 0 °C is only about 1 kcal/mol in favor of stacking, thus allowing reversible formation of an ordered helical chain, which may easily be disordered at higher temperatures or at constant temperature under the influence of external factors.

Two functionally distinct subpopulations of molecules were observed (Figure 6): one that was very sensitive to hydrolysis and repeatedly cleaved to its consumption (indicated by the empty arrow in Figure 6A) and the other that followed a slower kinetics (filled arrow). This behavior is compatible with the following mechanism: all of the molecules have similar conformation and accessibility but, once cleaved by a first-hit event, the hit molecule is rapidly cleaved to completion. This behavior could be explained by faster unstacking in the early part of the kinetics in shorter segments and/or faster processive hydrolysis from the induced extremities. Despite early reports (*23–25*) describing that the loss of the helical structure with an increase in temperature is not dependent upon chain length, thus essentially being a noncooperative process, evidence for cooperative stacking/unstacking effects was later reported (*26*). An alternative less likely interpretation of the cleavage pattern is that the CpC steps become more cleavable as they get closer to the A stretch because of context effects. Ascertaining the mechanism(s) responsible for the higher sensitivity of the CpC steps closer to the A stretch will require further analyses.

Whichever the mechanism leading to the rapid degradation of the polyC stretch after initial cleavages, the half-life of the full-length bicomposite oligo analyzed here is determined by its first-hit kinetics. This is safely calculated from the disappearance of the full-length molecules.

In these experimental conditions, the A-stretch component was more stable. The $T_0$ sample showed no signs of cleavages in this sequence portion (first lane in Figure 6A). The degradation pattern of the first time point ($T_{10}$) showed that the cleavage kinetics of the two sequence stretches (A stretch versus C stretch) were largely independent, that the cleavage of the A stretch was not progressive (in agreement with ref

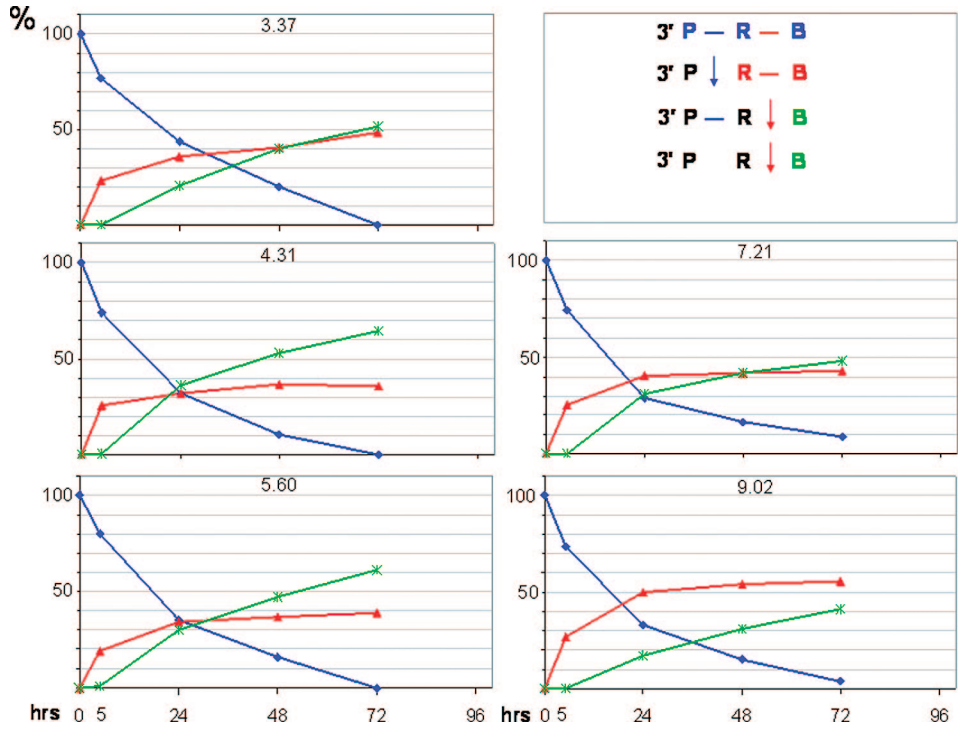


FIGURE 4: Degradation kinetics of 3′-CMP as a function of the pH, HPLC analysis. The experimental procedure and legend are the same as in Figure 1.

*25*), and that a "first-hit kinetics" condition applied. Values of 8 and 10 kcal/mol in favor of stacking were reported (refs *22* and *25*, respectively), indicating the higher tendency of the Poly A sequence to maintain an ordered stacked structure at least in the early moments of the treatment at 90 °C.

The Poly $A_{12}C_{12}$ sequence is composed of 11 5′-ApA-3′, 1 5′-ApC-3′, and 11 5′-CpC-3′ steps. The 5′-ApC-3′ step was cleaved less than both 5′-CpC-3′and 5′-ApA-3′.

*Mixed-Sequence RNA.* 5′-GGAAACGUAUCCUUUGG-GAG-3′. This sequence (dubbed "P1", *5*) contains the highly scissible base step 5′-UpA-3′ and, of the 16 possible combinations, only 5′-GpC-3′ and 5′-CpA-3′ (the other highly scissible step) are missing. This sequence was selected to have the highest possible number of sequence combinations and only one highly scissible site. The 5′-GpC-3′ step was not introduced to avoid sequence combinations that would lead to stable intrastrand structures (not detailed). As it is, this sequence lacks noticeable stable intrastrand structures, as determined by the standard Zuker analysis (*28*). With the exception of the cleavage of the 5′-UpA-3′ bond (indicated by an arrow on the left side of Figure 7A), the overall cleavage profile was rather homogeneous and only a slight preference was shown for the centrally located cluster of pyrimidine steps 5′-UpC-3′, 5′-CpC-3′, and 5′-CpU-3′ (Figure 7A).

The double bands appearing in correspondence of cleavages at advanced stages of the degradation process (indicated on the right side of Figure 7A) are due to successive steps of the hydrolytic process (*4, 29*). The cleavage of a 3′-phosphoester bond first results in the production of a 2′−3′-phosphate cyclic extremity (upper band in 5′-labeled oligomers), followed by the opening of the cyclic bond, yielding a nonresolved mixture of 2′- and 3′-monophosphate extremities (lower bands).

*Kinetics Aspects. The Hydrolytic Degradation of RNA in Water Is Preceded by a Lag Period.* Figures 5B, 6B, and 7B show the degradation kinetics at 90 °C in water of Poly A, Poly $A_{12}C_{12}$, and mixed-sequence P1 oligos, respectively.

The *average* half-life of the 3′-phosphoester bonds was calculated (see the Experimental Procedures) on the basis of the disappearance of the full-length molecules and the principle that this is a measure of independent first-hit events. In homogeneous-sequence molecules (as in Poly $A_{24}$), the calculated $t_{1/2}$ value corresponds to the half-life of homogenously cleaved (see Figure 5A) 3′-phosphoester bonds. The degradation kinetics of the Poly $A_{24}$ oligo at pH 5.5 and 6.2 are shown. The lag period is only observed for pH 5.5. Despite the relatively small acidity difference, at pH 6.2, the lag is lost. The explanation of this effect is given in the following section.

The two sequence blocks composing the Poly $A_{12}C_{12}$ oligo were cleaved with different kinetics, faster for the C stretch and slower for the A stretch (Figure 6A). In this case, the disappearance of the full-length molecules because of first-hit events was therefore mostly caused by cleavages of one of the relatively weaker 5′-CpC-3′ steps.

For the heterogeneous sequence 5′-GGAAACGUAUC-CUUUGGGAG-3′, the cleavage pattern did not show strong sequence-related cleavage biases (Figure 7A). Such cleavage homogeneity is not *a priori* expected but is *a posteriori* justified by the relevance of sequence-context effects (*10*) averaging out potential local cleavage differences, as confirmed by the inspection of the relatively homogeneous cleavage pattern (Figure 7A).

The kinetics of disappearance (percent, ordinate) of the full-length molecules (i.e., the kinetics of first-hit events) as a function of time (abscissa) at 90 °C shown in Figures 5B, 6B, and 7B revealed a lag of about 6 h before the onset of rapid degradation. In Figure 5B, consider only the open

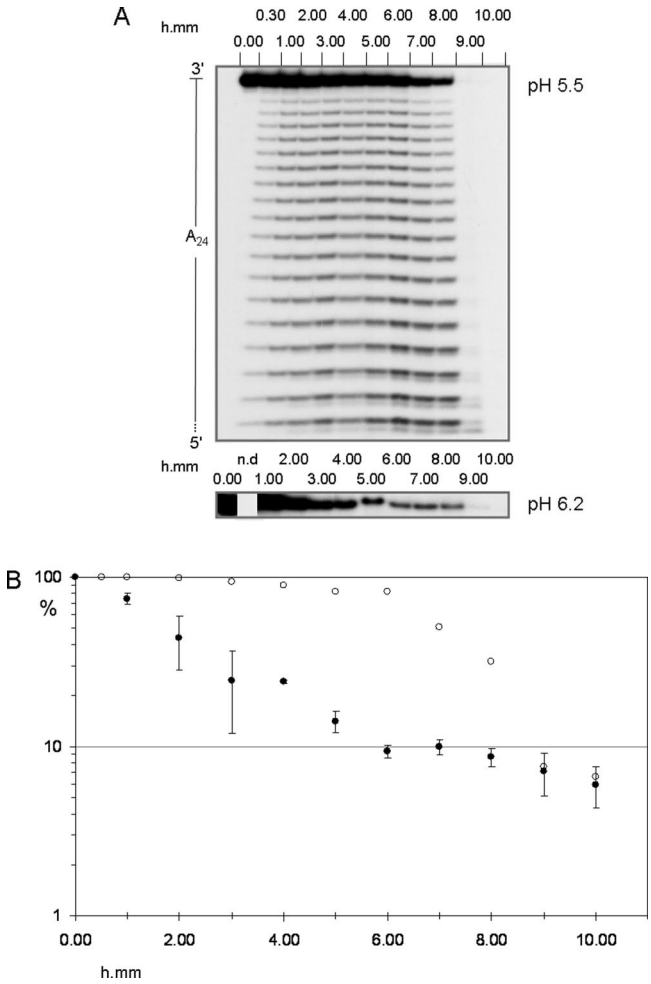


FIGURE 5: Kinetics of degradation of Poly $A_{24}$ in water at pH 5.5 and 6.2 and 90 °C. (A) 5′-Labeled oligo was treated (see the Experimental Procedures) for the period of time indicated on top of each lane (in hours) and analyzed in 16% acrylamide gel electrophoresis. After a lag period lasting for the first 6 h, rapid degradation started (see points at 7 and 8 h). Samples at 9 and 10 h were more than 90% degraded. The upper panel shows both the full-length molecules and the degradation ladder of the sample treated in water at pH 5.5. The lower panel shows only the full-length molecules of the sample treated in water at pH 6.2. (B) Quantitative analysis of the degradation of the full-length molecules reported in A. The molecules remaining intact are given as a percentage (ordinate) of the band present at each time point (abscissa) relative to the zero time control (C). ○, pH 5.5; ●, pH 6.2 (average of two experiments, with error bars).

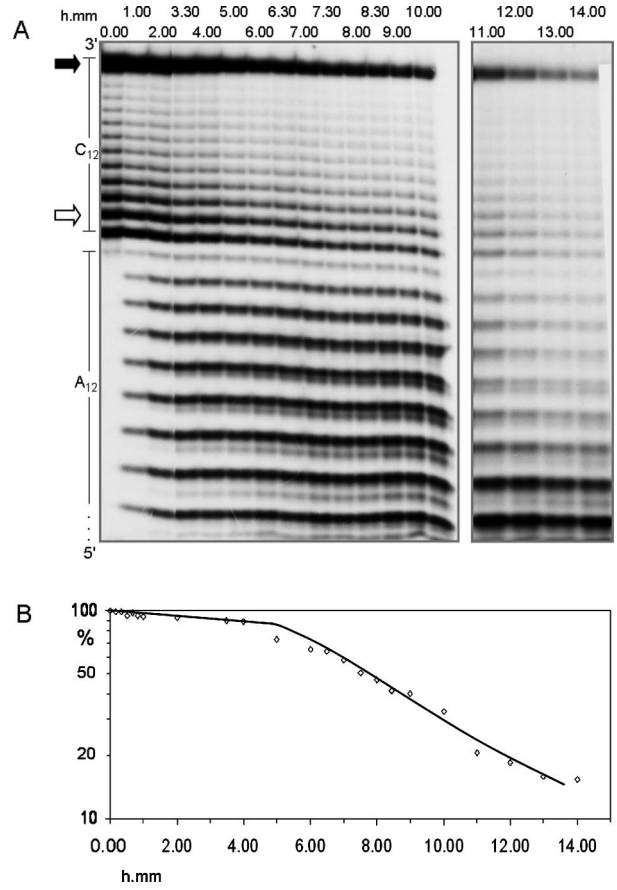


FIGURE 6: Kinetics of degradation of Poly $A_{12}C_{12}$ in water at pH 5.5 and 90 °C. The experimental procedure and representation are the same as the Poly $A_{24}$ analysis reported in Figure 5. The $C_{12}$ and $A_{12}$ moieties of the oligo are indicated (left, upper panel). A is split in two parts because the series of samples was analyzed in two parallel gels. The data points in B are taken from the experiment shown in A and from other similar experiments (not shown).

symbols. Filled symbols refer to the experiment described under Irreversibility. During this period, the RNA oligo polymers remained as intact full-length molecules. Operationally, the lag period was defined as the period during which 90% of the molecules remain full-lengthed.

In conclusion, RNA in water at pH 5.5 (90 °C) is resistant to hydrolysis for a relatively long time, after which it undergoes rapid degradation. This behavior is largely sequence-independent.

RNA stability in water at a different pH was also measured. The kinetics of degradation at pH 6.2 (90 °C) is shown (Figure 5B, ●). Data on the RNA kinetic sensitivity in a large range of pH values are given below.

*Irreversibility.* The lag resistance is not a reversible phenomenon. This was shown as follows:

(i) An RNA sample (conserved in water at −20 °C) was defrozen and treated for 6 h at 90 °C and then refrozen at −20 °C for 12 h. The sample was then reheated at 90 °C, and the kinetics of hydrolysis was analyzed with the standard procedure described in the previous paragraph. The results (Figure 7B, ▲) showed that the molecules are in this case hydrolyzed with a rapid-start kinetics, not undergoing again to the prehydrolysis lag period.

(ii) A dehydration step was introduced in a variant of this assay. After the 6 h treatment at 90 °C, RNA was ethanol-precipitated, then frozen, and treated as in (i). Also, in this case, the prehydrolysis lag was not observed.

Hysteresis effects in RNA conformation have been previously observed, and their basis was analyzed (*30, 31*). RNA meta-stability is based on acquired structures, from base stacking to complex foldings. In sequences that do not fold, as in our case, persistence of base stacking might contribute to stability for a certain period of time. However, the experiments described showed that stability, once lost, was not re-attained. This is only explained by a persistent, conceivably covalent modification (see below).

*cis versus trans.* The possibility was verified that the observed bipartite kinetics, consisting of a lag followed by a rapid transition to hydrolysis, could be due to trans-acting effects, as slow accumulation of degradation products up to a threshold level, or concentration-dependent effects. These

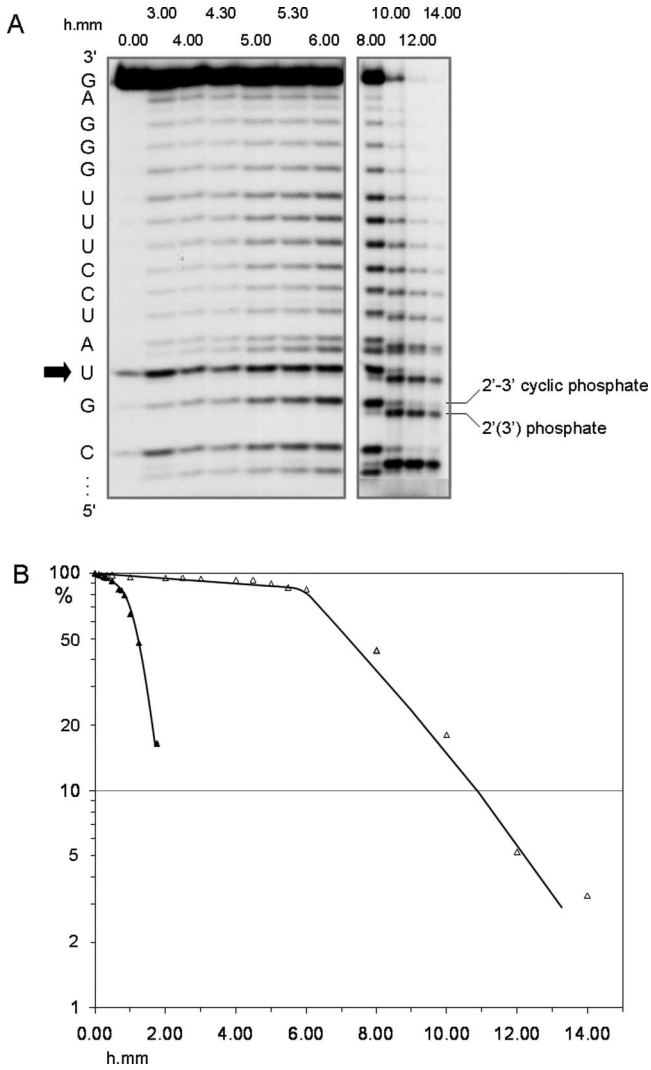


FIGURE 7: Kinetics of degradation of P1 in water at pH 5.5 and 90 °C. The experimental procedure and representation are the same as the Poly $A_{24}$ analysis reported in Figure 5. A is split in two parts because the series of samples was analyzed in two parallel gels, and only the relevant nonrepetitive parts of the analysis are shown. The arrow (left) points to the 5′-UpA-3′ labile step. The bands representing the 2′−3′-cyclic phosphate and the 2′ or 3′ free phosphate extremities are indicated (right, bottom). (B) △, the quantitative evaluation of the full-length molecules relative to the zero-time control; ▲, the kinetics of degradation of P1 in water after pretreatment (6 h) at 90 °C followed by freeze and thaw (see the text in Irreversibility).

possibilities were verified and discarded by the following experiments (not shown): (i) unlabeled P1 oligo was reacted in water at 90 °C for 1 min, 4 h, or 20 h and then added to a freshly dissolved 5′-labeled P1 sample. The kinetics of hydrolysis was then analyzed as usual (i.e., as in Figure 7). No modification of the degradation kinetics was observed. (ii) The same was repeated in the presence of unlabeled P1 oligo at 1×, 10×, and 50× concentration. Also, in this case, no modification of the degradation kinetics was occurred. Thus, the bipartite kinetics is caused by a cis-acting property.

*pH.* The analysis of the pH dependence of RNA stability was performed by measuring the residual amount of the full-length molecules (percent, ordinate) after 4 h in water at 90 °C at the indicated pH (abscissa) for Poly $A_{24}$ (Figure 8A), Poly $A_{12}$ $C_{12}$ (Figure 8B), and P1 (Figure 8C). Figure 8D compares the three profiles. The legend "depurination" in A refers to the data from Figure 2B). The two gel profiles in B show the cleavage pattern observed at the correspondingly arrowed pH values.

In conclusion, a well-defined sharp dependence of the RNA oligo stability on pH was observed, which varied as a function of the sequence composition.

*3. Half-Life of the 3′-Phosphoester Bond: Monomers versus Polymers. Temperature Effects.* The kinetics of hydrolysis in water was analyzed in detail as a function of the temperature in the mixed-sequence P1 oligo at 20, 30, 40, 50, 60, 70, 80, and 90 °C. The half-life values of the P1 RNA, calculated as described for the experiments reported in Figures 5−7, are shown for the whole range of temperatures in Figure 9. The figure compares the half-life of the 3′-phosphoester bond in the 3′-AMP monomer (■, data from Figure 3) with the half-life of the same bond in the P1 oligo (●). The error bar for the 80 °C temperature point is the average of six measurements, and the error bar for the 90 °C temperature point is the average of four measurements. All of the other points were measured once. The open dots indicate the duration of the lag period at each temperature. The comparison shows that at lower temperatures (up to 50 °C) the 3′-phosphoester bond was more stable in the monomer, while above 60 °C, the stability of this bond was markedly higher when embedded in the polymer. As evident, the difference is largely due to the lag period preceding the onset of hydrolytic degradation.

*Stability of the 3′-Phosphoester Bond in Formamide.* The half-lives of the 3′-phosphoester bond in the Poly $A_{24}$, Poly $A_{12}C_{12}$, and P1 oligos were determined in 100% formamide. The degradation reactions (not shown) strictly followed first-order kinetics, with no hints of lag periods. The calculated half-lives in formamide are Poly $A_{24} = 2.7 \times 10^3$ min, Poly $A_{12}C_{12} = 5.5 \times 10^3$ min, and P1 $= 7.7 \times 10^3$ min. The order of increasing resistance is Poly $A_{24}$ < Poly $A_{12}C_{12}$ < P1. The sensitivity of nucleic bases in formamide at high temperature was determined (*32, 33*). The order of increasing resistance is G ≥ A > C ≫ T, with G being degraded in minutes, while pyrimidines are largely more resistant. After base degradation, the phosphodiester chain is cleaved by a $\beta$-elimination mechanism (*7*). The same order of increasing resistance was respected in the oligos analyzed here: the polypurine Poly $A_{24}$ is cleaved faster that purine−pyrimidine Poly $A_{12}C_{12}$, while the mixed sequence is the most resistant. The half-life of the same bond was also determined at various water/formamide ratios at the temperatures of 20, 30, 50, 60, 70, 80, or 90 °C. The data are reported in Figure 10. The cleavage mechanism of the 3′-phosphoester bond in formamide is described in ref *46*.

Figure 10 compares the half-lives in formamide of the 3′-phosphoester bond in the monomer (black and white symbols) and in the three oligomers (colored symbols) analyzed at 90 °C. Also, in the nonaqueous medium, the bonds are more and sequence-selectively resistant in the polymers than in the monomers.

## DISCUSSION

The root of the "RNA world" boils down to the origin of RNA as an informational polymer. This origin is not understood.

It is not known how the nucleic bases were made available in sufficient concentrations and in acceptably equilibrated

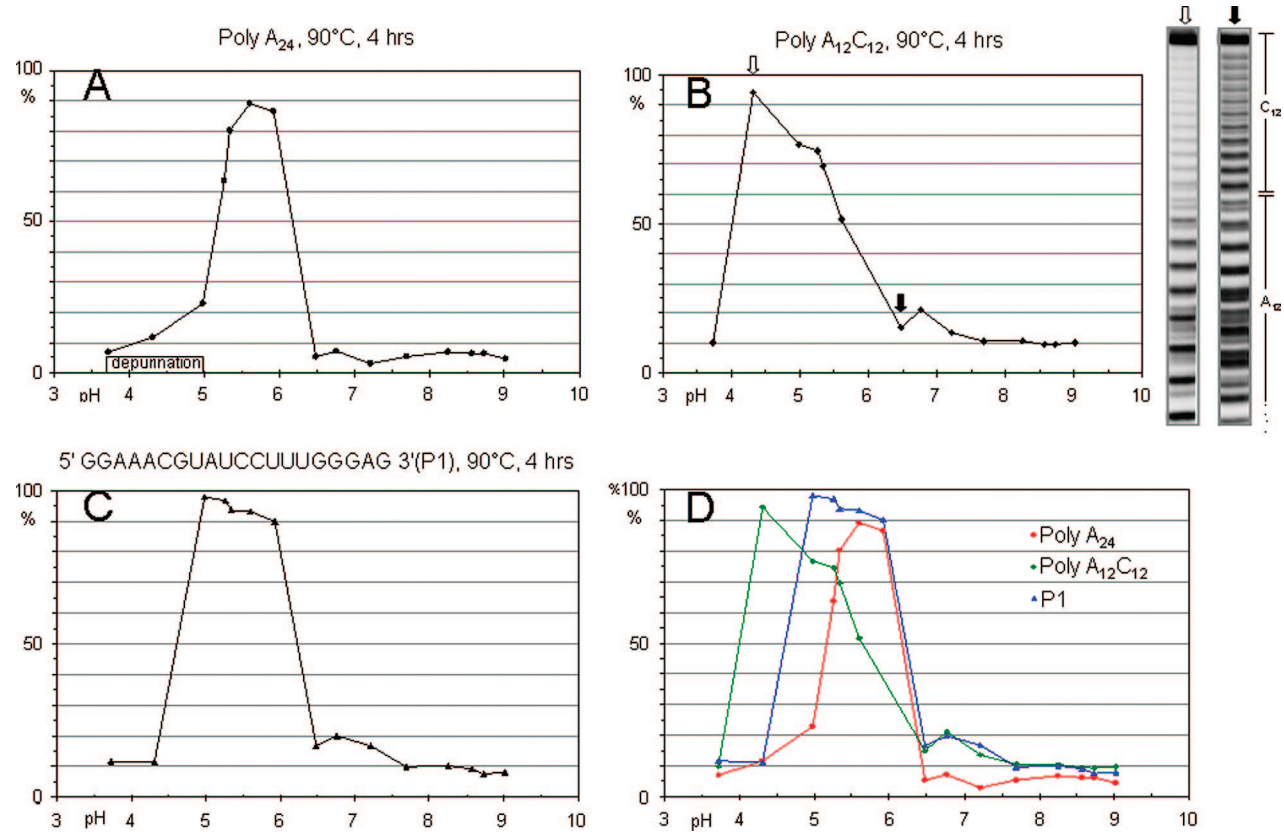


FIGURE 8: Stability of RNA as a function of pH. Each data point shows the percentage of full-length molecules (ordinate) after 4 h at 90 °C in Tris-HCl-buffered water at the indicated pH (abscissa). (A) Poly $A_{24}$, (B) Poly $A_{12}C_{12}$, and (C) mixed-sequence P1. In B, two gel profiles are shown resulting from treatment at the pH values indicated by the corresponding arrows. D shows the comparison of the pH-dependent stabilities of Poly $A_{24}$, Poly $A_{12}C_{12}$, and P1 oligos reported in A−C, respectively.

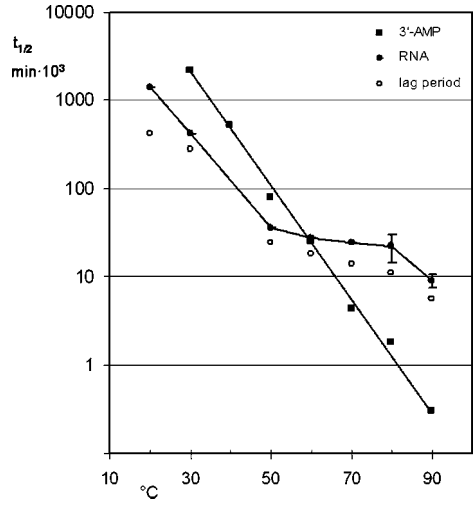


FIGURE 9: Stability of the 3′-phosphoester bond when present in 3′-AMP (■, data from Figure 3) and in the oligomer P1 (●). In the oligomer data set, each point represents the half-life (ordinate) calculated in degradation analyses similar to those represented in Figures 5−7, performed at the indicated temperature (abscissa). Open dots indicate the duration of the lag period at the specified temperature (see the text).

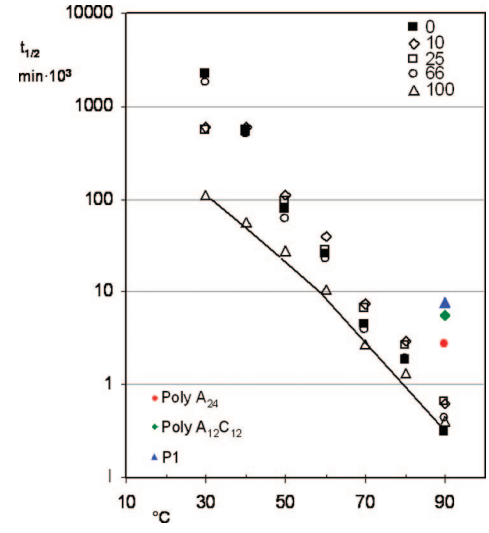


FIGURE 10: Stability of the 3′-phosphoester bond when present in 3′-AMP (black and white symbols) in formamide/water solutions. The formamide/water percent composition of the various solutions analyzed is specified in the upper right corner. The average half-lives of the 3′-phosphoester bond in the three oligomers studied (data described in the text of section 3) are shown by the colored symbols (as specified in the lower left corner).

pools nor how they chemically evolved into nucleosides nor which activation mechanism allowed the monomeric units to polymerize in a process that in a pre-enzymatic world would have necessarily been spontaneous and self-sustaining. It is not known whether this phrasing of the problem only corresponds to an *a posteriori* logic and other different mechanisms played a kick-starting role. Among these alternative mechanisms: the role of mineral surface-based syntheses (*34–37*) or the possibility that RNA and/or RNA-like molecules evolved from simpler polymeric forms (*38–40*).

It is not known whether evolutionary space was explored by molecules replicating in aqueous surroundings or if replication/evolution was only made possible for molecules

encompassed in confined microenvironments providing favored thermodynamic niches.

Nevertheless, one point is uncontroversial: the basic requirement of the first molecules was to survive for a period long enough to allow for their reproduction and, hence, their evolution. The founding phenotype of the pregenetic molecules was stability. Limiting for simplicity our analysis to RNA as we know it and to the solvent as water, we asked the question: does RNA have properties that favor its stability in water and that at the same time determine/favor sequence-related evolutionary effects? In considering the conditions in which pregenetic polymers could spontaneously polymerize, replicate, and evolve, stability of the polymeric form is of major concern.

We have shown that the stability of 3′ mononucleotides in water decreases with an increasing temperature according to a linear function (Figure 3). Degradation of the 3′ mononucleotide is due to both the primary cleavage of the 3′-phosphoester bond and the cleavage of the $\beta$-glycosidic bond (followed by $\beta$-elimination) (*7*), eventually leading to complete degradation of the nucleotide (Figure 1). Between pH 3.5 and 8.7, the overall half-life of the 3′-phosphoester bond (as resulting from the sum of the two degradative reactions) was observed to be largely pH-independent (Figure 2A). Depurination was prominent between pH 3.7 and 5.0 (Figure 2B).

The half-life of the 3′-phosphoester bond in oligonucleotides was on the contrary markedly pH- and sequence-dependent (Figure 8), and its decrease as a function of the temperature was not linear (Figure 9). A direct comparison of the half-lives of the 3′-phosphoester bond in the monomer with that of the same bond embedded in the polymer revealed that a large area of enhanced resistance to hydrolysis exists, favoring the polymer bond at temperatures higher than 60 °C (Figure 9). The increased stability of the polymer lasted at 90 °C for 5–6 h. During this period, the polymer was not attacked but prepared for the onset of rapid hydrolysis (Figures 5−7). We discuss below the possibility that these properties favor at the same time the polymeric over the monomeric state and the evolution of sequence complexity.

*Factors Affecting the Cleavage. Stacking and Hydrogen Bonding.* Factors that enhance transesterification have been studied extensively, and the effect of the base sequence on the reactivity of phosphodiester bonds has been determined (*2, 10, 14*). The effect of base composition on the stability of RNA phosphodiester bonds has been frequently attributed to stacking interactions between the adjacent nucleic acid bases (*11–13*).

A conformational explanation for this effect was indicated (*13*) consisting of the fact that strong stacking hinders the cleavage of the intervening phosphodiester bond by preventing the attacking 2′-OH, the phosphorus atom, and the departing 5′ oxygen to adopt the colinear conformation necessary for efficient transesterification (as reviewed in ref *3*). However, an inverse correlation trend of the reactivity of phosphodiester bonds with the stacking free-energy profiles for all of the 16 natural ribonucleoside monophosphates in aqueous solution (*14*) was not observed (*10*). The evidence for the importance of a local stacking interaction among neighboring bases in determining the reactivity (mostly on the basis of dinucleotides data *10*) is contradictory. Stacking farther in the molecule was suggested as a major determinant of the overall structure of the oligomers (*11–13*) based on the fact that the reactivity is not particularly sensitive to the nearest neighborhood of the scissile bond. The hydrogen-bonding network related to the hydration pattern was indicated as the effector of this sequence context effect (*10, 12, 41*). A particularly telling example of sequence context is that of the 5′-UpA-3′ phosphodiester bond (*10*), which as such is not significantly less stable than the other phosphodiester bonds but whose reactivity is strongly affected by surrounding sequences. Other similar effects were also described (*ibidem*).

It was concluded (*10*) that the reactivity of phosphodiester bonds within RNA oligonucleotides having no defined secondary structure is strongly dependent upon the base sequence of the substrate only at low temperatures, whereas no such differences are observed with dinucleotide monophosphates or tetrameric oligonucleotides. The reason for the marked sensitivity of the cleavage of phosphodiester bonds to the base sequence was attributed to the fact that the oligonucleotide chain may adopt a structure, stabilized by intramolecular interactions, such as base stacking or hydrogen bonding, that either facilitates or retards transesterification. Base stacking is known to stabilize the A-form helical conformation of single-stranded oligonucleotides (*42–44*). As for the cytosines, in a cleavage analysis of cytosine-rich sequences, it was reported that, consistent with the known self-stacking tendency of the cytosine bases (*44*), the component of the C-rich stretches stack upon each other, which forces the scissile phosphodiester bond in an unfavorable conformation. However, no or a very small free-energy barrier was observed for the unstacking of the py−py ribodinucleoside monophosphates (*14*).

The oligonucleotides that exhibit rate retardations in all likelihood adopt, because of base stacking and hydrogen bonding, a structure that hinders the free rotation of the phosphodiester bond and hence the reaction by an in-line mechanism (*10*).

However, the data discussed below indicate that it is unlikely that stacking and hydrogen bonding confer the essentially complete resistance at 90 °C observed to last for more than 5 h.

*Temperature Effects.* The stacking–unstacking process was shown to be very temperature-dependent, and the transition barrier was found to be lower at higher temperatures (*20*). A free-energy landscape, which describes the stacking–unstacking process of a ribotrinucleoside diphosphate has been calculated (*21*). Consistent with these data, the formation of a semistable ordered structure in oligonucleotides is lost at high temperature, a condition in which the base-stacking sequence-related reactivity differences almost completely disappear (*10*). At 90 °C, the cleavage rate becomes almost independent of the base sequence.

*Lag Period and pH Effect.* The kinetics of degradation of the three oligos tested is peculiar: a lag period, which is similar for the three sequences analyzed, during which the RNA backbone length does not change, followed by rapid degradation. The lag lasts for several hours at 90 °C and is lost at pH $<4$ and $>6$. Given the inconsistency of the occurrence of first-hit events at 90 °C after several hours being due to the persistence of a protective stacked conformation, no definitive explanation for this effect can be provided at present. However, the existence and character-

istics of the lag period can be interpreted mechanistically by the following default reasoning: the kinetics and mechanisms for the cleavage and isomerization of the phosphoester bonds of RNA by Brønsted acids and bases were thoroughly analyzed and reviewed (*45*). The pH−rate profiles for transesterifications have been determined over a wide range of acidity, extending from concentrated acid solutions to concentrated aqueous alkalines. Under neutral or alkaline pH conditions, the dominant pathway for RNA degradation is an internal phosphoester transfer reaction that is promoted by specific base catalysis (*11*). In most instances, the identities of the nucleotide bases that flank the target RNA linkage have a negligible effect on the p$K_a$ of the nucleophilic 2′-hydroxyl group and only have a minor effect on the maximal rate constant for the transesterification reaction (as reviewed in ref *11*). Alkaline conditions favor specific base catalysis, in which the 2′-hydroxyl group is deprotonated by hydroxide to generate the more nucleophilic 2′-oxyanion group. The ensuing reaction is the primary pathway for the uncatalyzed degradation of RNA under typical cellular conditions (*6*).

Facile transesterification also occurs under strong acid conditions (*45*). With reaction conditions below pH 6, specific base catalysis becomes a minor mechanism relative to the competing mechanism of specific acid catalysis for RNA transesterification (*45*).

A bell-shaped pH−rate profile was reported, with the minimum reactivity centering at pH 5 (*45*). This shape was interpreted to indicate the involvement of four kinetically distinct terms in the cleavage reaction, with the monoanionic phosphodiester being largely predominant at pH 4−6. As pointed out (*11*), around these pH values, both specific base and specific acid catalyses are near a minimum (*45*) and cleavage by a depurination/$\beta$-elimination mechanism (*7*) becomes increasingly significant.

One is therefore left with a chemical environment encompassed between pH 4 and 6, in which the onset or the absence of depurination or of other reactions leading to base degradation or removal become relevant. In our experimental setup at 90 °C, depurination of 3′-AMP levels off after $0.3 \times 10^3$ min (Figure 1), being more prominent between pH 3.37 and 5.24 (Figure 2B). The loss of the pyrimidine base cytosine or the corresponding nucleoside cytidine from 3′-CMP (Figure 4) is not pH-dependent and occurs in $\sim 1 \times 10^3$ min.

The average duration of the lag period (Figures 5−67) corresponds to the time required for depurination and depyrimidination (Figures 1 and 4). $\beta$-Elimination follows. Thus, by default, a limited area of pH values is left, in which neither specific base nor specific acid catalysis occur and the RNA backbone resists degradation. On the acidic side, above pH 3.37 and below pH 5.24, depurination further limits pure purine RNA stability, as seen in Poly $A_{24}$ (Figure 8A).

A pH-determined niche is thus defined, in which RNA stability strictly depends upon its sequence.

## CONCLUSIONS

At the molecular level, in a prebiotic acellular context, the founding phenotype of the developing system of informational molecules is stability. Along with the ability to reproduce, selection necessarily favored molecules able to keep, for a longer time, their macromolecular information. On the basis of this assumption, we have analyzed the stability of ribo oligomers and compared it to that of the constituent monomers. The results showed that, at well-defined pH and temperature conditions, polymers are favored. We hypothesize that this property conferred to the polymer a sufficient Darwinian edge over its constituent monomers not only to allow for its very survival in the polymeric form but also to provide a phenotype for evolution. The complex sequence resists more, in terms of time and in wider environmental conditions, thus being favored.

## REFERENCES


1. van Holde, K. (1980) *The Origins of Life and Evolution* (Halvorson, H. O., and van Holde, K. E, Eds.) p 31, Alan R. Liss, Inc., New York.
2. Perreault, D. M., and Anslyn, E. V. (1997) Unifying the current data on the mechanism of cleavage-transesterification of RNA. *Angew. Chem., Int. Ed. Engl. 36*, 432–450.
3. Soukup, G. A., and Breaker, R. R. (1999) Nucleic acid molecular switches. *Trends Biotechnol. 17*, 469–476.
4. Soukup, G., and Breaker, R. (1999) Relationship between internucleotide linkage geometry and the stability of RNA. *RNA 5*, 1308–1325.
5. La Neve, P., Altieri, F., Fiori, M. E., Scaloni, A., Bozzoni, I., and Caffarelli, E. (2003) Purification, cloning, and characterization of XendoU, a novel endoribonuclease involved in processing of intron-encoded small nucleolar RNAs in *Xenopus laevis*. *J. Biol. Chem. 278*, 13026–13032.
6. Jarvinen, P., Oivanen, M., and Lonnberg, H. (1991) Interconversion and phosphoester hydrolysis of 2′,5′- and 3′,5′-dinucleoside monophosphates: Kinetics and mechanisms. *J. Org. Chem. 56*, 5396–5401.
7. Lindhal, T. (1993) Instability and decay of the primary structure of DNA. *Nature 362*, 709–715.
8. Smith, K. C., and Allen, F. W. (1953) The liberation of polynucleotides by the alkaline hydrolysis of ribonucleic acid from yeast. *J. Am. Chem. Soc. 75*, 2131–2133.
9. Lane, B. G., and Butler, G. C. (1959) The exceptional resistance of certain oligoribonucleotides to alkaline degradation. *Biochim. Biophys. Acta 33*, 281–283.
10. Kaukinen, U., Lyytikäinen, S., Mikkola, S., and Lönnberg, H. (2002) The reactivity of phosphodiester bonds within linear single-stranded oligoribonucleotides strongly dependent on the base sequence. *Nucleic Acids Res. 30*, 468–467.
11. Li, Y., and Breaker, R. R. (1999) Kinetics of RNA degradation by specific base catalysis of transesterification involving the 2′-hydroxyl group. *J. Am. Chem. Soc. 121*, 5364–5372.
12. Bibillo, A., Figlerowicz, M., and Kierzek, R. (1999) The nonenzymatic hydrolysis of oligoribonucleotides. VI. The role of biogenic polyamines. *Nucleic Acids Res. 27*, 3931–3937.
13. Kierzek, R. (1992) Nonenzymatic hydrolysis of oligoribonucleotides. *Nucleic Acids Res. 20*, 5079–5084.
14. Norberg, J., and Nilsson, L. (1995) Stacking free energy profiles for all 16 natural ribodinucleoside monophosphates in aqueous solution. *J. Am. Chem. Soc. 117*, 10832–10840.
15. Norberg, J., and Nilsson, L. (1998) Solvent influence on base stacking. *Biophys. J. 74*, 394–402.
16. Luo, R., Gilson, H. S. R., Potter, M. J., and Gilson, M. K. (2001) The physical basis of nucleic acid base stacking. *Biophys. J. 80*, 140–148.
17. Newcomb, L. F., and Gellman, S. H. (1994) Aromatic stacking interactions in aqueous solution: Evidence that neither classical hydrophobic effects nor dispersion forces are important. *J. Am. Chem. Soc. 116*, 4993–4994.
18. Friedman, R. A., and Honig, B. (1995) A free energy analysis of nucleic acid base stacking in aqueous solution. *Biophys. J. 69*, 1528–1535.
19. Pohorille, A., Burt, S. K., and MacElroy, R. D. (1984) Monte Carlo simulation of the influence of solvent on nucleic acid base associations. *J. Am. Chem. Soc. 106*, 402–409.
20. Norberg, J., and Nilsson, L. (1995) Temperature dependence of the stacking propensity of adenylyl-3′,5′-adenosine. *J. Phys. Chem. 99*, 13056–13058.

21. Norberg, J., and Nilsson, L. (1996) A conformational free energy landscape of ApApA from molecular dynamics simulations. *J. Phys. Chem. 100*, 2550–2554.
22. Norberg, J., and Nilsson, L. (1996) Influence of adjacent bases on the stacking−unstacking process of single-stranded oligonucleotides. *Biopolymers 39*, 765–768.
23. Brahms, J., Maurizot, J. C., and Michelson, A. M. (1967) Conformation and thermodynamic properties of oligocytidylic acids. *J. Mol. Biol. 14*, 465–480.
24. Brahms, J., Michelson, A. M., and van Holde, K. E. (1966) Adenylate oligomers in single- and double-strand conformation. *J. Mol. Biol. 15*, 467–488.
25. van Holde, K. E., Brahms, J., and Michelson, A. M. (1965) Base interactions of nucleotide polymers in aqueous solution. *J. Mol. Biol. 12.*, 726–739.
26. Kaukinen, U., Venalainen, T., Lonnberg, H., and Perakyla, M. (2003) The base sequence dependent flexibility of linear single-stranded oligoribonucleotides correlates with the reactivity of the phosphodiester bond. *Org. Biomol. Chem. 1*, 2439–2447.
27. Leng, M., and Felsenfeld, G. (1966) A study of polyadenylic acid at neutral pH. *J. Mol. Biol. 15*, 455–466.
28. Zuker, M. (1989) On finding all suboptimal foldings of an RNA molecule. *Science 244*, 48–52.
29. Kuusela, S., and Lönnberg, H. (1994) Metal-ion-promoted hydrolysis of polyuridylic acid. *J. Chem. Soc., Perkin Trans. 2*, 2301.
30. Revzin, A., Neumann, E., and Katchalsky, A. (1973) Metastable secondary structures in ribosomal RNA: A new method for analyzing the titration behavior of rRNA. *Biopolymers 12*, 2353–2383.
31. Pinder, J. C., Staynov, D. Z., and Gratzer, W. B. (1974) Properties of RNA in formamide. *Biochemistry 13*, 5367–5373.
32. Negri, R., Costanzo, G., Saladino, R., and Di Mauro, E. (1996) One-step, one-lane chemical DNA sequencing by *N*-methylformamide in the presence of metal ions. *BioTechniques 21*, 910–917.
33. Saladino, R., Mincione, E., Crestini, C., Negri, R., Di Mauro, E., and Costanzo, G. (1996) Mechanism of degradation of purine nucleosides by formamide. Implications for chemical DNA sequencing procedures. *J. Am. Chem. Soc. 118* (24), 5615–5619.
34. Cairns-Smith, A. G. (1966) The origin of life and the nature of the primitive gene. *J. Theor. Biol. 10*, 53–88.
35. Cairns-Smith, A. G., Hall, A. J., and Russell, M. J. (1992) Mineral theories of the origins of life and an iron sulfide example. *Origins Life Evol. Biosphere 22*, 161–180.
36. Franchi, M., Ferris, J. P., and Gallori, E. (2003) Cations as mediators of the adsorption of nucleic acids on clay surfaces in prebiotic environments. *Origins Life Evol. Biosphere 33*, 1–16.
37. Winter, D., and Zubay, G. (1995) Binding of adenine and adenine-related compounds to the clay montmorillonite and the mineral hydroxylapatite. *Origins Life Evol. Biosphere 25*, 61–81.
38. Benner, S. A., and Sismour, A. M. (2005) Synthetic biology. *Nat. Rev. Genet. 6*, 533–543.
39. Bean, H. D., Anet, F. A., Gould, I. R., and Hud, N. V. (2006) Glyoxylate as a backbone linkage for a prebiotic ancestor of RNA. *Origins Life Evol. Biosphere 36*, 39–63.
40. Nielsen, P. E., Egholm, M., Berg, R. H., and Buchardt, O. (1991) Sequence-selective recognition of DNA by strand displacement with a thymine-substituted polyamide. *Science 254*, 1497–1500.
41. Bibillo, A., Figlrowicz, M., Ziomek, K., and Kierzek, R. (2000) The nonenzymatic hydrolysis of ribonucleotides. VII. Structural elements affecting hydrolysis. *Nucleosides Nucleotides 19*, 977–994.
42. Suurkuusk, J., Alvarez, J., Freire, E., and Biltonen, R. (1977) Calorimetric determination of the heat capacity changes associated with the conformational transitions of polyriboadenylic acid and polyribouridylic acid. *Biopolymers 16*, 2641–2652.
43. Filimonov, V. V., and Privalov, P. L. (1978) Thermodynamics of base interaction in $(A)_n$ and $(A\cdot U)_n$. *J. Mol. Biol. 122*, 465–470.
44. Freier, S. M., Hill, K. O., Dewey, T. G., Marky, L. A., Breslauer, K. J., and Turner, D. H. (1981) Solvent effects on the kinetics and thermodynamics of stacking in polycytidylic acid. *Biochemistry 20*, 6198–6206.
45. Oivanen, M., Kuusela, S., and Lönnberg, H. (1998) Kinetics and mechanisms for the cleavage and isomerization of the phosphodiester bonds of RNA by Brønsted acids and bases. *Chem. Rev. 98*, 961–990.
46. Saladino, R., Crestini, C., Ciciriello, F., Di Mauro, E., and Costanzo, G. (2006) Origin of informational polymers: Differential stability of phosphoester bonds in ribo monomers and oligomers. *J. Biol. Chem. 281*, 5790–5796.
47. Saladino, R, Crestini, C, Busiello, V, Ciciriello, F, Costanzo, G, and Di Mauro, E. (2005) Origin of informational polymers differential stability of 3′- and 5′-phosphoester bonds in deoxy monomers and oligomers. *J. Biol. Chem. 280*, 35658–35669.

BI7021014